2015 International Symposium on Nonlinear Theory and its Applications
NOLTA2015, Kowloon, Hong Kong, China, December 1-4, 2015

Polarization chaos from free-running laser diode: peculiarities and applications

Martin Virte†, Marc Sciamanna‡, Hugo Thienpont† and Krassimir Panajotov†,*

†Brussels Photonics Team (B-Phot), Dept. of Applied Physics and Photonics,
Vrije Universiteit Brussel, Pleinlaan 2, 1050 Brussel, Belgium.
‡OPTEL Research Group and Laboratoire Matriaux Optiques Photoniques et Systmes (LMOPS) EA-4423,
CentraleSupelec - Université de Lorraine, 2 rue Edouard Belin, F-57070 Metz, France.
∗ Institute of Solid State Physics, 72 Tzarigradsko Chaussee Blvd., 1784 Sofia, Bulgaria.
Email: mvirte@b-phot.org

Abstract—In this contribution, we focus on the double-scroll polarization chaos dynamics that can be generated in free-running vertical-cavity surface-emitting laser diodes. At first glance, the two scrolls of the chaotic attractor seems to be symmetrical, but we report here clear experimental indications that the dynamics is in fact asymmetric: in particular, we unveil a peculiar statistical evolution of the dynamics. Physically, we demonstrate that the symmetry breaking mechanism corresponds to a misalignment of the phase and amplitude anisotropies in the laser cavity. By introducing this additional feature in the theoretical spin-flip model for VCSELs, we can then efficiently reproduce all the dynamics observed experimentally. Finally, we address the problematic of exploiting polarization chaos in chaos-based applications. We make a proof-of-concept demonstration of a random bit generation scheme based on polarization chaos, and despite non-optimal characteristics of the dynamics, we successfully obtain performances competitive with other state-of-the-art systems.

1. Introduction

Semiconductor lasers are classified as class B lasers [1, 2], i.e. devices typically exhibiting two degrees of freedom, and therefore behave as damped nonlinear-oscillators. As a result, to generate a chaotic output with a laser diode at least one additional degree of freedom is required. In practice, external perturbation or forcing such as optical injection, feedback or modulation are used to induce chaotic behaviour in the lasers. But an additional degree of freedom can also appear directly inside the device itself: we recently showed that the polarization mode competition in vertical-cavity surface-emitting lasers (VCSELs) could indeed lead to chaotic dynamics [3].
The dynamics and the corresponding bifurcation scenario can be accurately reproduced in the spin-flip model (SFM) framework for VCSELs [4, 5]. When increasing the injection current, the linear polarization (LP) stable at threshold is first destabilized by a pitchfork bifurcation which creates two elliptically polarized (EP) states. These two steady-states are symmetrical with respect to the LP at threshold and experience the same bifurcations although with a different orientation of the polarization. Two supercritical Hopf bifurcations create symmetrical limit cycles, and then the system follows a period-doubling route to chaos. As a result, two single-scroll chaotic attractors oscillating around the two unstable EP co-exist. As they grow in the phase space along with the injection current, they finally merge to form a double-scroll attractor [3, 6].

2. Symmetry breaking and dynamical impact

As described above, in the SFM framework the system exhibits a perfect symmetry between the two EP orientations and therefore between the two scrolls of the chaotic attractor. However, this perfect symmetry does not match the experimental observations.
First, in the chaotic devices we observed a peculiar bistability between two limit cycles oscillating around the two EP orientations [7]. Although the co-existence of the two limit cycles was expected, the difference of amplitude and frequency, along with the clear hysteresis cycle between the two periodic solutions, does not correspond to a symmetrical system. Similarly, statistical features of the polarization chaos dynamics also support this interpretation. As displayed in Fig. 1, the average dwell-time - i.e. the time between two successive jumps between the two EP orientations - shows, in some devices, a strongly asymmetric evolution for increasing injection currents. Not only one EP orientation is preferred over the other - we observe a difference in the average dwell-time up to 2 orders of magnitude -, but this affinity is changed for different levels of current, accompanied by a relatively strong increase of the average dwell-time. At larger currents, the difference between the two sides of the attractor are reduced as the dwell-time tends toward the nanosecond level for both orientations. At this point, it is important to notice that this behaviour is not observed in all chaotic devices as mentioned in [8]. Indeed some VCSELs show statistical features much closer to the simple exponential decrease observed for the symmetric case.

Theoretically, the spin-flip model (SFM) used so far

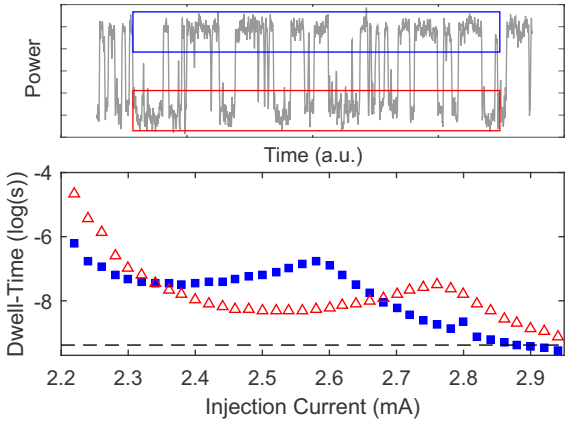

Figure 1: (Top) Typical time-series of the polarization chaos dynamics projected at 45° of the LP at threshold. The blue and red frame highlight the upper and lower levels of the time trace corresponding to the two EP orientations. (Bottom) Strongly asymmetrical evolution of the dwell-time statistics of the dynamics for increasing injection currents. The blue squares (red empty triangles) show the evolution for the upper (lower) level of the time-series.

and with which polarization chaos dynamics and its corresponding bifurcation scenario can be accurately reproduced is not sufficient any longer. Within this framework the two EP orientations are perfectly symmetric and therefore no differences can arise between the two sides of the chaotic attractor. In order to enable the emergence of asymmetrical features we therefore need a symmetry breaking mechanism. As described in [9], a misalignment of the phase and amplitude anisotropy can efficiently play this role, and thus the equation of SFM becomes:

$$\begin{aligned}
\dot{R}_+ =&\kappa(N+n-1)R_+ - R_-\left(\overline{\gamma_a}cos(\phi)+\overline{\gamma_p^+}sin(\phi)\right)\\
\dot{R}_- =&\kappa(N-n-1)R_- - \overline{\gamma_a}R_+cos(\phi)+\overline{\gamma_p^-}R_+sin(\phi)\\
\dot{\phi} =&2\kappa\alpha n + \overline{\gamma_a}sin(\phi)\left(\frac{R_-}{R_+}+\frac{R_+}{R_-}\right)+\left(\overline{\gamma_p^-}\frac{R_+}{R_-}-\overline{\gamma_p^+}\frac{R_-}{R_+}\right)cos(\phi)\\
\dot{N} =&\gamma(\mu - N -(N+n)R_+^2-(N-n)R_-^2)\\
\dot{n} =&-\gamma_s n-\gamma((N+n)R_+^2-(N-n)R_-^2)
\end{aligned}$$

with $R_\pm$ the electrical field amplitude for the right (+) and left (-) circular polarizations, ϕ the phase difference between the two circular polarizations, N the normalized total carrier population and n the normalized carrier population difference between the two reservoirs. κ is the electric field decay rate in the cavity, γ is the carrier decay rate and γ_s is the spin-flip relaxation rate that accounts for the spin homogenization of the spin up and spin down carrier populations. α is the linewidth enhancement factor, μ is the normalized injection current. Finally, the phase anisotropy or birefringence is γ_p whereas γ_a is the amplitude anisotropy. For simplicity, we define the effective anisotropies: $\overline{\gamma_p^\pm} = \gamma_p \mp sin(2\theta)\gamma_a$ and $\overline{\gamma_a} = cos(2\theta)\gamma_a$. θ is defined as the angle between the axis of maximum frequency and the axis of maximum losses. Unless stated otherwise, we use the following parameters: $\kappa = 600\,ns^{-1}$, $\alpha = 3$, $\gamma_a = -0.7\,ns^{-1}$, $\gamma_p = 5\,ns^{-1}$, $\gamma = 1\,ns^{-1}$ and $\gamma_s = 100\,ns^{-1}$.

In Fig. 2, we show the impact of such anisotropy misalignment on the bifurcation diagram of the system: we see that the pitchfork bifurcation is immediately destroyed for $\theta \neq 0$, hence forming one main branch connected to the LP state stable at threshold and a second branch created by a saddle-node bifurcation. As a result of this separation, we observe that the two Hopf bifurcations creating the limit cycles - which will be later be degenerated to single-scroll chaotic attractors - appear at different injection currents. In fact, we observe a shift of the complete bifurcation scenario, thus leading e.g. to the limit cycle bistability highlighted in [7].

For some set of parameters, we also observed a restabilization of the two limit cycles within the region of polarization chaos. Interestingly, these cycles are only marginally stable and a tiny amount of spontaneous emission noise is sufficient to kick the system out of their basin of attraction. Yet, their existence influences the statistics of the dynamics and typically leads to an increase of the dwell-time. Then considering an asymmetric case, the stability range of the two restabilized limit cycles will shift, therefore impacting only one side of the chaotic attractor at a time. As a result, an asymmetrical evolution similar to the one displayed in Fig.

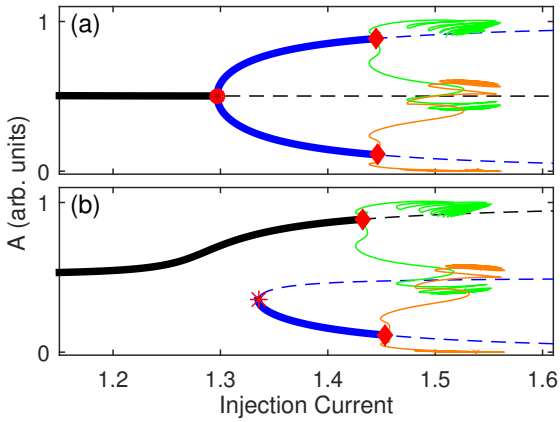

Figure 2: Evolution of the bifurcation diagram in the $A = R_+^2/(\mu-1)$ versus increasing injection current plane without (top, a) and with (bottom, b) anisotropy misalignment. The black line is the steady-state stable at threshold while the blue line shows the EP steady-state(s). Red circles, diamonds and stars represent pitchfork, Hopf and saddle-node bifurcations respectively. The green and orange curves are the limit cycles created by the two Hopf bifurcations on the upper and lower EP orientations respectively. Thick (thin dashed) lines indicate stable (unstable) steady-states. For simplicity, no stability information is displayed for limit cycle branches.

1 will be obtained. In practice, with the parameters used in this contribution and a noise level of only $\beta_{sp} = 4.10^{-9}$ - which is few orders of magnitude lower than what can be expected in a VCSEL device -, we demonstrated a good agreement with the experimental results [8].

3. Applications of the polarization chaos dynamics

Obviously, from the applied physics viewpoint, the main interest of generating a chaotic output without the need for external perturbation or forcing is the simplicity of the resulting physical setup as in e.g. [10, 11]. But a quick comparison with state-of-the-art solutions for chaos-based applications highlights some potential drawbacks of the polarization chaos dynamics such as its low-dimension and its limited bandwidth [12, 13, 14]. Indeed these characteristics have been identified as crucial properties to ensure high-performances for chaos-based applications, and it therefore casts some doubts about the potential of polarization chaos-based systems.
To verify these assumptions, we put in place a random bit generation (RBG) scheme based on polarization chaos from a free-running laser diode. As expected the physical setup presented in Fig. 3(a) is extremely simple: the chaotic polarization fluctuations are just converted in intensity fluctuations using a polarizer and then recorded using a photodiode and an analog-to-digital converter. For simplicity, the collimation lens, the fiber coupler sending the optical signal to the photodiode and the optical isolator preventing back reflections from the fiber front facet are not represented. All the details of the setup and the equipment used can be found in [15]. It is also important to remark that the optical power received by the photodiode has been adjusted to ensure that the 8-bit range of the ADC is fully covered. Nevertheless the 8-bit output cannot directly be exploited as a random sequence; a suitable post-processing technique need to be considered similarly to what is done in other schemes [11, 13, 16]. One simple solution consist in keeping only some of the least significant bits (LSBs) of each data point of the time-series. Unfortunately in our case this method lead to a biased output bit sequence even at low sampling rate and considering only 1-LSB. As a result, we decided to use a slightly more complex technique where we compare the recorded time-series with a time-shifted version of itself. In practice, with a time-shift of 0.25 ns and keeping 5-LSBs at a sampling rate of 20 GSamples/s, the output bit sequence pass all the NIST and dieHard statistical tests [17, 18]; details can be found in [15]. This result therefore suggest that performances up to 100 Gbps could be obtained with the suggested scheme which is competitive with the latest report.

Besides the performance itself, it is important to understand why we were able to obtain such result. Indeed, we successfully obtain a random sequence from a low-dimensional chaotic dynamics recorded using a small-bandwidth photodiode, while so far, most schemes have been optimized to increase the system bandwidth without detailed consideration of the dynamics peculiaritiesOliver2013. In [15], we demonstrate that the filtering from the acquisition electronics actually plays the role of a first randomness extraction stage. Although this is quite unintuitive, the low-pass filter leads to a significant increase of the 1-bit entropy [14] as the largely correlated oscillations around the two wings of the chaotic attractor - shown in Fig. 3(b) - are filtered out. This is mainly due to the fact that the largest finite-time Lyapunov exponent is small when the system oscillates around one EP orientation while much larger values appear close to the switching point. The random-like hopping between the two sides of the chaotic attractor are therefore the events generating most of the randomness. Hence, in this case, focusing on how to harvest these events will have a stronger impact on the performances than an increase of the dynamics bandwidth.

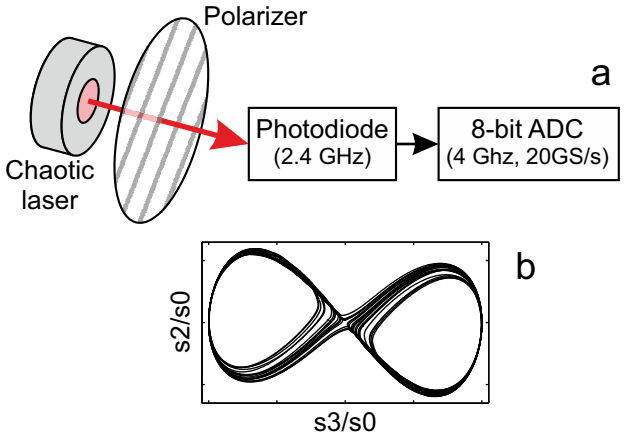

Figure 3: (a) Schematic of the physical part of the proposed random bit generation scheme based on polarization chaos. Using a polarizer oriented, the chaotic polarization fluctuations are transformed into an intensity signal which is then recorded using a low-bandwidth photodiode (2.4 GHz) followed by an ADC. (b) Representation of the attractor of polarization chaos projected in the Stokes parameter space.

4. Conclusion

The observation and identification of polarization chaos represent a significant step forward in our understanding of the nonlinear dynamics of VCSELs. It confirms the validity of the SFM framework for VCSELs, and provides a deeper insight on the impact of anisotropies on VCSEL dynamics. Of course, these results also motivate further theoretical and experimental investigations which would allow us to fully understand VCSEL nonlinear behaviour.
On the other hand, we also demonstrate competitive performances for RBG applications using this chaotic dynam-

ics. Despite dynamical features seemingly non-optimal for chaos-based applications, the proposed scheme showed an interesting potential in line with the most recent reports [16, 19, 13]. In addition, our work highlights anew the importance of considering the intrinsic dynamical properties of the chaotic signal to improve current systems further. Finally, these results also encourage testing polarization chaos dynamics for other chaos-based applications.

Acknowledgments

The authors acknowledge support from the METHUSALEM program of the Flemish Government, FWO-Vlaanderen, the Interuniveristy attraction poles program of the Belgian Science Policy Office (IAP P7-35 photonics@be), the conseil rgional de Lorraine and the Suplec Foundation.

References

[1] F. T. Arecchi, G. L. Lippi, G. P. Puccioni, and J. R. Tredicce, "Deterministic chaos in laser with injected signal," Opt. Commun. **51**, 308 (1984).

[2] M. Sciamanna and K. Shore, "Physics and applications of laser diode chaos," Nature Photonics **9**, 151–162 (2015).

[3] M. Virte, K. Panajotov, H. Thienpont, and M. Sciamanna, "Deterministic polarization chaos from a laser diode," Nature Photon. **7**, 60–65 (2012).

[4] M. San Miguel, Q. Feng, and J. V. Moloney, "Light-polarization dynamics in surface-emitting semiconductor lasers," Phys. Rev. A **52**, 1728 (1995).

[5] J. Martin-Regalado, F. Prati, M. San Miguel, and N. B. Abraham, "Polarization properties of vertical-cavity surface-emitting lasers," IEEE J. Quantum Electron. **33**, 765 (1997).

[6] M. Virte, K. Panajotov, and M. Sciamanna, "Bifurcation to nonlinear polarization dynamics and chaos in vertical-cavity surface-emitting lasers," Phys. Rev. A **87**, 013834 (2013).

[7] M. Virte, M. Sciamanna, E. Mercier, and K. Panajotov, "Bistability of time-periodic polarization dynamics in a free-running VCSEL," Optics Express **22**, 6772 (2014).

[8] M. Virte, E. Mirisola, M. Sciamanna, and K. Panajotov, "Asymmetric dwell-time statistics of polarization chaos from free-running VCSEL," Optics letters **40**, 1865–1868 (2015).

[9] M. Travagnin, "Linear anisotropies and polarization properties of vertical-cavity surface-emitting semiconductor lasers," Phys. Rev. A **56**, 4094 (1997).

[10] T. Harayama, S. Sunada, K. Yoshimura, P. Davis, K. Tsuzuki, and A. Uchida, "Fast nondeterministic random-bit generation using on-chip chaos lasers," Physical Review A **83**, 031803 (2011).

[11] A. Argyris, S. Deligiannidis, E. Pikasis, A. Bogris, and D. Syvridis, "Implementation of 140 Gb/s true random bit generator based on a chaotic photonic integrated circuit," Opt. Express **18**, 18763 (2010).

[12] A. Uchida, K. Amano, M. Inoue, K. Hirano, S. Naito, H. Someya, I. Oowada, T. Kurashige, M. Shiki, S. Yoshimori, K. Yoshimura, and P. Davis, "Fast physical random bit generation with chaotic semiconductor lasers," Nature Photon. **2**, 728 (2008).

[13] N. Oliver, M. C. Soriano, D. W. Sukow, and I. Fischer, "Fast random bit generation using a chaotic laser: approaching the information theoretic limit," IEEE J. Quantum Electron. **49**, 910 (2013).

[14] T. Mikami, K. Kanno, K. Aoyama, A. Uchida, T. Ikeguchi, T. Harayama, S. Sunada, K.-I. Arai, K. Yoshimura, and P. Davis, "Estimation of entropy rate in a fast physical random-bit generator using a chaotic semiconductor laser with intrinsic noise," Phys. Rev. E **85**, 016211 (2012).

[15] M. Virte, E. Mercier, H. Thienpont, K. Panajotov, and M. Sciamanna, "Physical random bit generation from chaotic solitary laser diode," Optics Express **22**, 17271 (2014).

[16] T. Yamazaki and A. Uchida, "Performance of Random Number Generators Using Noise-based Super-Luminescent Diode and Chaos-based Semiconductor Lasers," IEEE J. Sel. Top. Quantum Electron. **19**, 0600309 (2013).

[17] G. Marsaglia, "DieHard: a battery of tests of randomness," Tech. rep., Florida State University (1996).

[18] A. Rukhin, J. Soto, J. Nechvatal, M. Smid, E. Barker, S. Leigh, M. Levenson, M. Vangel, D. Banks, A. Heckert, J. Dray, and S. Vo, "A Statistical Test Suite for Random and Pseudorandom Number Generators for Cryptographic Applications - Special Publication 800-22 Rev1a," Tech. Rep. April, National Institute of Standards and Technology (2010).

[19] X.-Z. Li and S.-C. Chan, "Heterodyne Random Bit Generation Using an Optically Injected Semiconductor Laser in Chaos," IEEE J. Quantum Electron. **49**, 829 (2013).